1 **Mitigation in Multiple Effects of Graphene Oxide Toxicity in Zebrafish**

2 **Embryogenesis Driven by Humic Acid**

3

4 Yuming Chen, Chaoxiu Ren, Shaohu Ouyang, Xiangang Hu*, Qixing Zhou*

5

6 Key Laboratory of Pollution Processes and Environmental Criteria (Ministry of
7 Education)/Tianjin Key Laboratory of Environmental Remediation and Pollution
8 Control, College of Environmental Science and Engineering, Nankai University,
9 Tianjin 300071, China

10
11
12
13
14
15
16
17
18
19
20
21
22
23
24
25
26
27
28

29 Prepared for ***Environmental Science & Technology***
30 Number of pages: 18
31 Number of figures: 18
32 Number of tables: 2

33
34
35
36
37
38
39
40
41
42
43

44 **MATERIALS AND METHODS**

45 **Zebrafish maintenance**

46 For all of the experiments performed in this study, zebrafish embryos (AB strain)
47 were maintained at 26 − 30 °C in a buffered solution consisting of 60 mg/L Instant
48 Ocean Salts in reverse osmosis-purified water under a 14 h/10 h light/dark cycle. The
49 zebrafish were fed brine shrimp twice daily.

50

51 **Hatching, heartbeat and malformations**

52 The emergence of larval fish from the chorion was considered successful hatching.
53 The embryos were transferred to 0.016 M tricaine for anesthetization. The embryonic
54 and larval structures were imaged using light microscopy (Olympus ZL 61, Olympus,
55 Japan), and the incidence of pericardial edema was recorded. The heartbeat was
56 assessed via continuous observation for 5 min at room temperature.

57

58 **Adsorption of nanomaterials on plastic and glass walls**

59 To investigate the sorption of nanomaterials in the plastic walls of 96-well plates and
60 the glass walls of petri dishes, 10 ml 100 mg/L graphene oxide (GO) with or without
61 10 mg/ L humic acid (HA) is spiked into 96-well plastic plates and 35-mm diameter
62 glass petri dishes, respectively, and incubated under dark for 24 h. The concentrations
63 of GO before and after the incubation were detected using external standard method
64 on a UV−vis spectrophotometer (Purkinje General T90, Purkinje General, China) at λ
65 = 230 nm.

66 **Hypoxic microenvironment of embryos**

67 Prior to use, the sensor was polarized overnight at –0.80 V to remove oxygen. Then,
68 six embryos were incubated for 24 h in E3 solution containing 100 mg/L GO, with or
69 without HA, and then fixed using low melting point agarose (1%). The hypoxic
70 microenvironment was detected using an oxygen microsensor. A CAL300 calibration
71 chamber was employed to calibrate Profix 3105 software, and measurements were
72 performed in the samples at 50 μm intervals. The depth of analysis ranged from 100
73 to 250 μm, consistent with the interspace between the chorion and the embryo. The
74 sensor was held at each sampling site for 5 s.

75

76 **Transmission electron microscopy (TEM)**

77 Embryos were fixed in 2.5% glutaraldehyde overnight at 4 °C, then rinsed using
78 phosphate−buffered saline (PBS, pH 7.2), postfixed with 1% osmium tetroxide, and
79 dehydrated through a graded ethanol series. The samples were subsequently
80 embedded in resin (Spurr's low viscosity resin) and sectioned using an Ultracut UCT
81 (Leica EM UC7, Germany). Images were obtained via TEM (Hitachi HT7700, Japan)
82 at 80 kV.

83

84 **Biochemical constituents of the embryos**

85 The chorions were removed from the embryos using forceps at 24 hpf. Both the
86 dechorionated embryos and the chorions were freeze dried for 24 h. Then, the samples

were thoroughly mixed with completely dried KBr (100 mg) and subjected to a pressure of 5 $\times 10^6$ pa in an evacuated die to produce a clear transparent disc with a diameter of 13 mm and thickness of 1 mm. FT-IR spectra in the region from 4,000 − 400 cm^{-1} were recorded in a Bruker Tensor 27 infrared spectrometer. For each spectrum, 100 interferograms providing a spectral resolution of 4 cm^{-1} were co-added. The absorption intensities of the peaks were calculated via the baseline method. Each sample was scanned with three different pellets under identical conditions, all of which produced identical spectra. These replicates were averaged and then used for further analysis. The spectra were analyzed using Origin 8.5 and Peak Fit_ v4.12 software.

EPR measurements

To measure the generation of hydroxyl radicals ($^{\bullet}OH$) from the interactions between GO and the chorions, electron paramagnetic resonance (EPR) was performed using 5,5−dimethyl−1−pyrroline−N−oxide (DMPO) as a trapping agent. Embryos were incubated in GO100 and GO100−HA with 75 mM DMPO from 10 to 12 hpf. The yield of $^{\bullet}OH$ was followed by measuring the intensity of DMPO/$HO^{\bullet}$ adduct EPR signals. All X−band EPR spectra were collected at room temperature (296 K) using a Magnettech MiniScope 400 EPR spectrometer (Germany) operated at a microwave frequency of 9.4 GHz and a magnetic field modulation frequency of 100 kHz. The spectrometer was controlled using MiniScope Control software.

Tracing the uptake of GO *in vivo*

10 mL GO at 100 μg/mL and 100 μL fluorescein isothiocyanate (FITC) at 1 mg/mL were mixed under sonication for 10 min. The FITC-labeled GO (GO-FITC) solution was filtered using a dialysis membrane (Solarbio, MWCO 3.5-5 KD) to remove the free FITC. Finally, the real-time monitoring of GO-FITC transport with or without HA (10 mg/L) in 16 hours post fertilization (hpf) embryos was performed via laser scanning confocal microscopy (Olympus, FV1000, Japan).

Mitochondrial membrane potential loss

The mitochondrial membrane potential loss was measured using the lipophilic cationic dye 5,5,6,6−tetrachloro−1,1,3,3−tetraethylbenzimidazolylcarbocyanine iodide (JC−1). JC−1 selectively enters mitochondria and changes color from red to green with loss of the membrane potential. At 72 hpf, embryos were collected, washed with E3 medium, incubated with 6 μM JC−1 for 1 h and then thoroughly washed in culture medium alone. Subsequently, the embryos were transferred to 0.016 M tricaine for anesthetization. A fluorescence microscope (Olympus X71, Olympus, Japan) with CellSens Standard 1.6 software was used to detect the fluorescence intensity. The double excitation wavelengths were 475 nm and 520 nm.

Determination of 8-hydroxy-2-deoxy guanosine levels

For this assay, 30 fish were used and two replicates were performed (60 fish per

130 treatment). Embryos were exposed to GO (100 mg/L) with or without HA until 96 hpf.
131 Then, the fish were collected, flash frozen, and stored at −80 °C until analysis. DNA
132 was extracted using the DNeasy Blood & Tissue Easy Kit (Qiagen, Valencia, CA) and
133 quantified using a T90 spectrophotometer (Purkinje General, China). The production
134 of 8-OHdG was determined using a Synergy 4 microplate reader (Bio Tek, USA) and
135 absorbance at λ = 405 nm. 8-OHdG concentrations were normalized to DNA mass.
136
137 **Protein carbonyls**
138 30 fish were used and two replicates were performed (60 fish per treatment). Embryos
139 were exposed to GO (100 mg/L) with or without HA until 96 hpf. Then, the fish were
140 collected, flash frozen, and stored at −80 °C until analysis. The protein carbonyls that
141 reflect oxidative stress in embryos were quantified using the Bradford assay and an
142 Oxy ELISA oxidized protein quantitation kit. As the kit's instruction manual, the
143 absorbance at 450 nm was measured using a TU-1901 UV-vis spectrophotometer
144 (Purkinje General, China).
145
146 **RESULTS**
147
148 Table S1. The main chemical bonds of humic acid*.

Bond energy	Chemical bonds	Radio (%)
284.8	C-C/C-C sp^2	67.7
286.5	C-O/C-N	10.45
288.5	O-C=O	12.98
292.4	C=C	8.84

149 *, Data from the signals of C1s.
150
151 Table S2. General band assignments of the FT−IR spectra of zebrafish embryos.

Peak number	Peak position (cm^{-1})	Vibrational Assignments	Corresponding biomolecules
1	2957	the asymmetric stretching of CH_3 mode	Lipids
2	2853	symmetric stretching modes of CH_2	Lipids
3	1681/1637	C=O stretching of amide Ⅰ	Proteins
4	1543	N−H bending of amide Ⅱ	Proteins
5	1110	PO_2^- stretching	RNA
6	1025	PO_2^- stretching	DNA

152
153

154

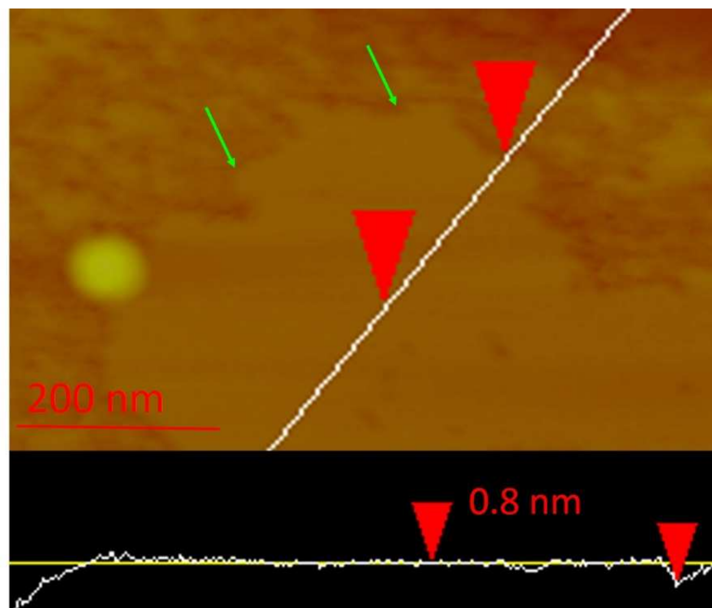

155 **Figure S1.** Atomic force microscopy images of graphene oxide. Green arrows
156 indicates the zigzag edges of graphene oxides nanosheets.

157

158

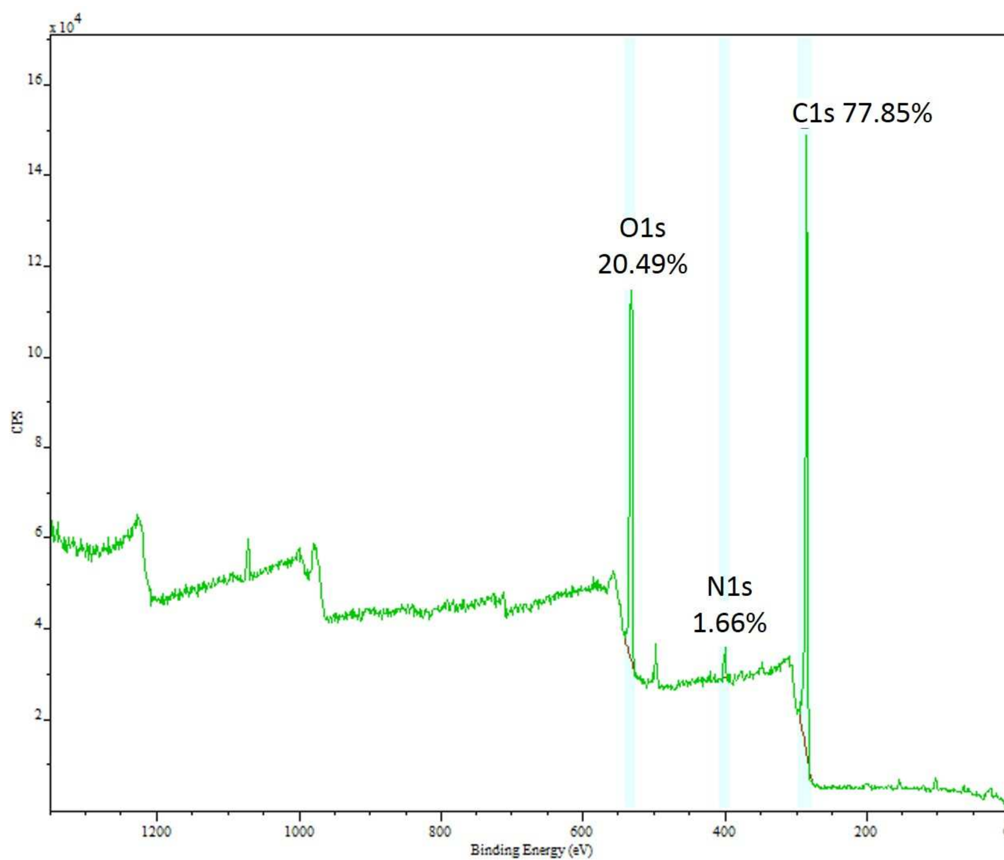

159

160 **Figure S2.** Full X-ray photoelectron spectra of humic acid.

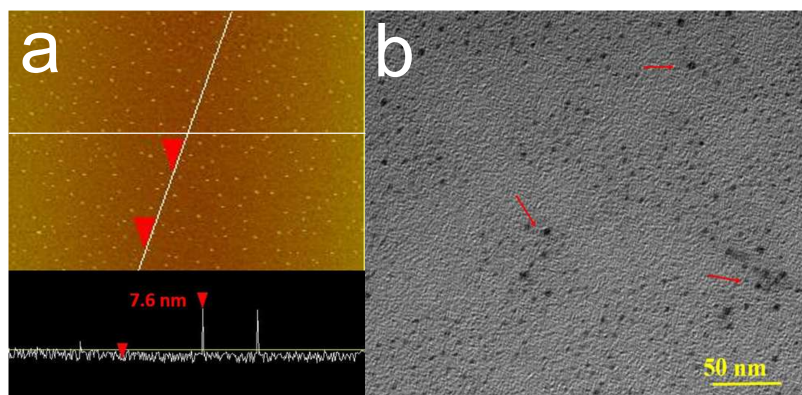

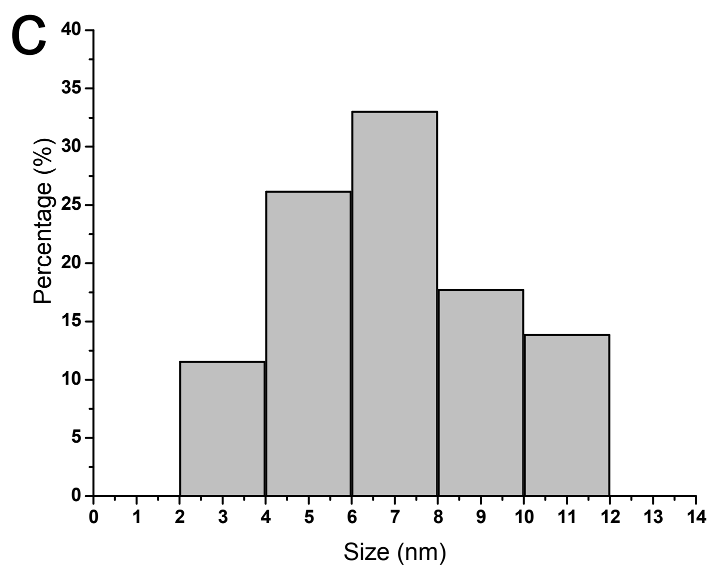

161

162 **Figure S3.** AFM, TEM and the size distribution of HA. (a) AFM. (b) TEM. (c) Size
163 distribution. Six images and 200-300 particles per images were measured. TEM,
164 transmission electron microscopy; AFM, atomic force microscopy.

165

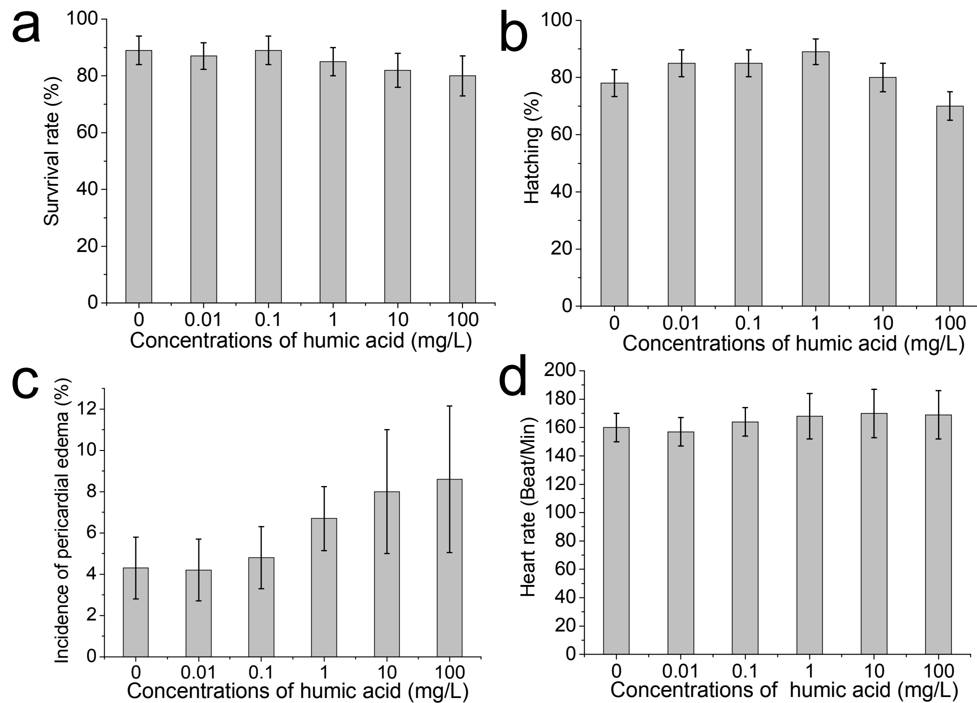

166

167 **Figure S4.** Effects of HA on zebrafish embryogenesis at 72 hpf. (a) Survival rate. The
168 experiment was conducted three times with 40 embryos each time. (b) Hatching rate.
169 The experiment was conducted three times with 24 embryos each time. (c) Incidence
170 of pericardial edema. Each experiment was conducted three times with 40 embryos
171 each time. (d) Heartbeat. Each experiment was conducted twice with six embryos
172 each time. HA, humic acid. *****, significant level at $p < 0.05$ compared with the control
173 (0 mg/L HA).

174

175

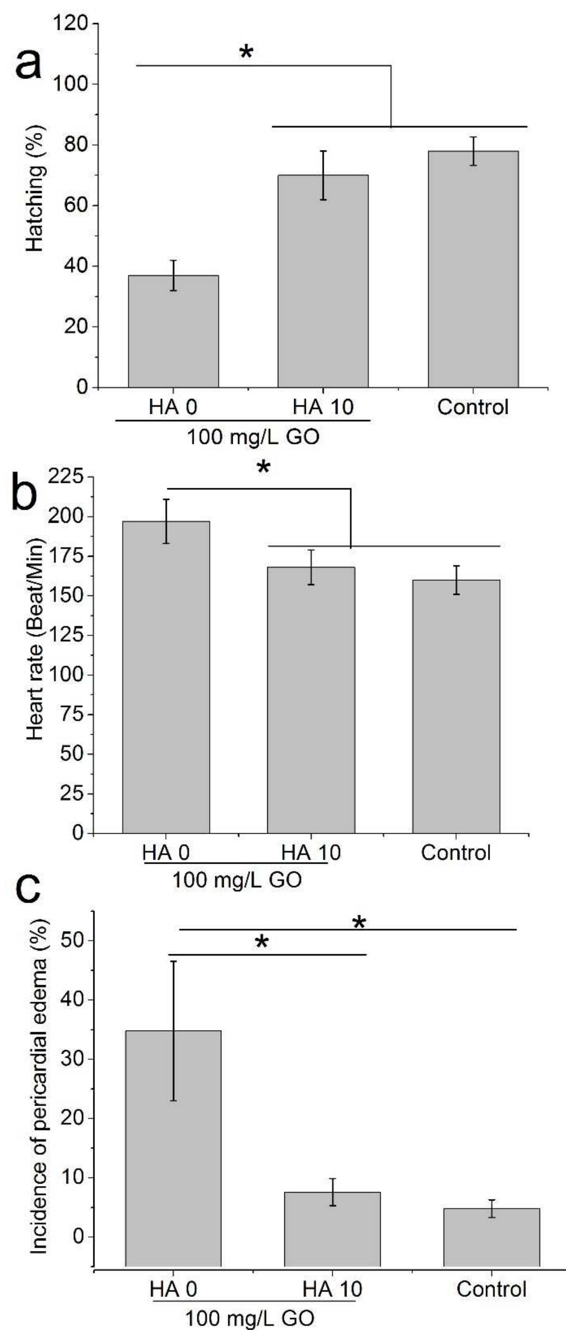

176 **Figure S5.** Effects of GO and GO−HA on zebrafish embryogenesis at 72 hpf. (a)
177 Hatching rate. The experiment was conducted three times with 24 embryos each time.
178 (b) Heartbeat. The experiment was conducted twice with six embryos each time. (c)
179 Incidence of pericardial edema. The experiment was conducted three times with 40
180 embryos each time. *, significant at the $p < 0.05$ level compared with the control. HA
181 0: 0 mg/L humic acid; HA 10: 10 mg/L humic acid; GO: graphene oxide; GO−HA:
182 mixed solution of graphene oxide and humic acid.
183

184

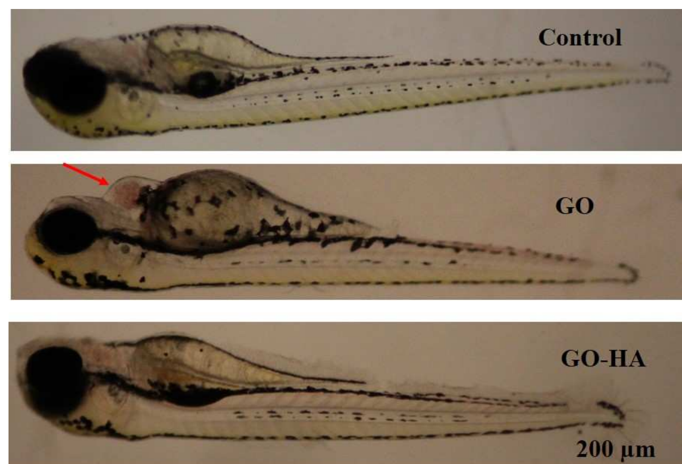

185 **Figure S6.** Representative images of malformed embryos. Red arrows denote
186 pericardial edema. GO, graphene oxide at 100 mg/L; HA, humic acid at 10 mg/L.
187

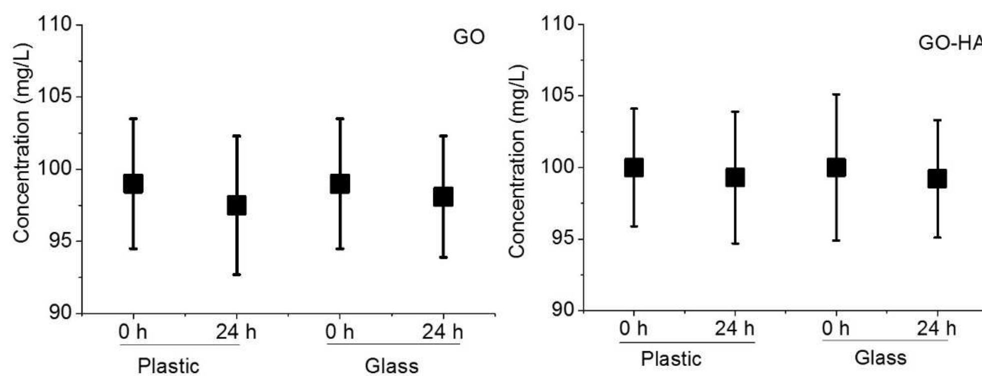

188

189 **Figure S7.** Sorption of GO and GO-HA on plastic wells within 96-well plates and
190 glass walls of petri dish. 0 h, the initial concentration of nanomaterials. 24 h, the
191 terminal concentration of nanomaterials. GO, graphene oxide, 100 mg/L. HA, humic
192 acid, 10 mg/L. *****, significant level at $p < 0.05$ compared nanomaterial concentrations
193 at 24 h with the initial concentrations of nanomaterials at 0 h.
194

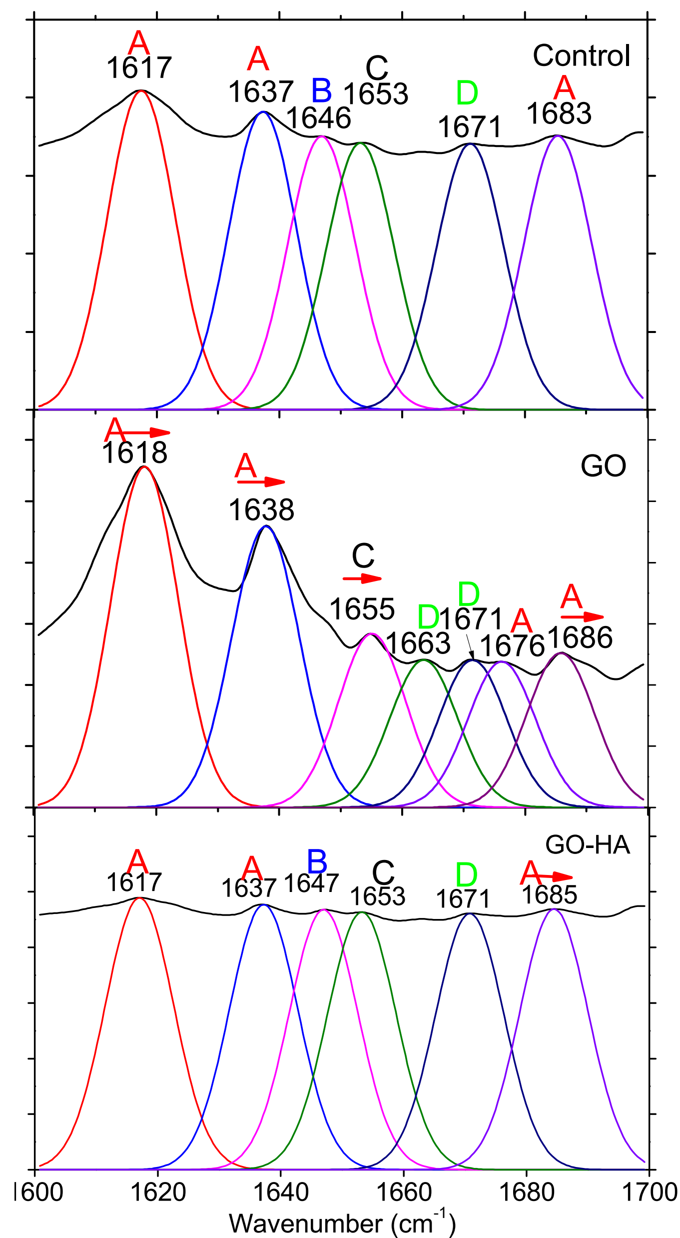

195

196 **Figure S8.** Protein secondary structures of the zebrafish chorion. The red arrows
197 indicate the variation of peak positions. Capital A, B, C and D indicate the protein
198 secondary structures of β−sheets, random coils, α−helixes, and turns and bends,
199 respectively. GO, 100 mg/L graphene oxide; HA, 10 mg/L; HA, humic acid. There
200 were 25 embryos in each treatment group, n = 3.

201

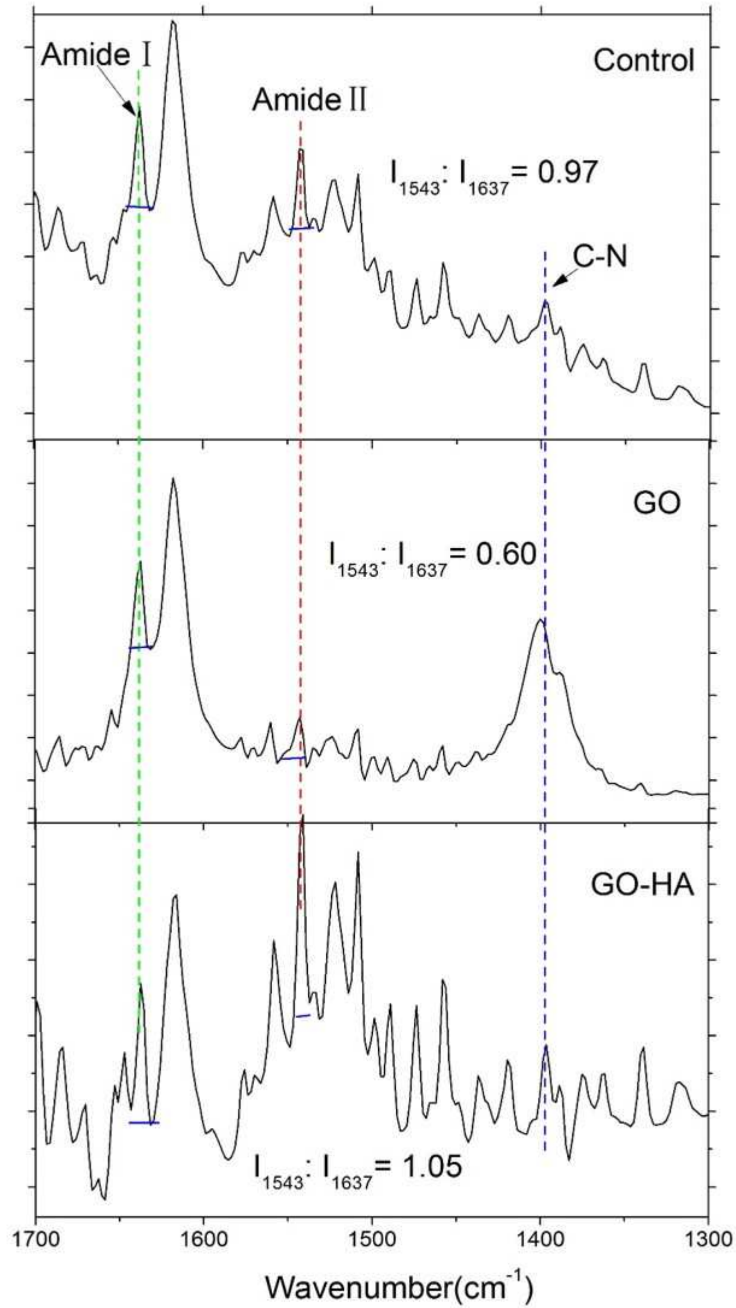

202

203 **Figure S9.** FT−IR spectra of chorions treated with GO and GO−HA. GO, graphene
204 oxide at 100 mg/L; HA, humic acid at 10 mg/L. There were 25 embryos in each
205 treatment group, n = 3.

206

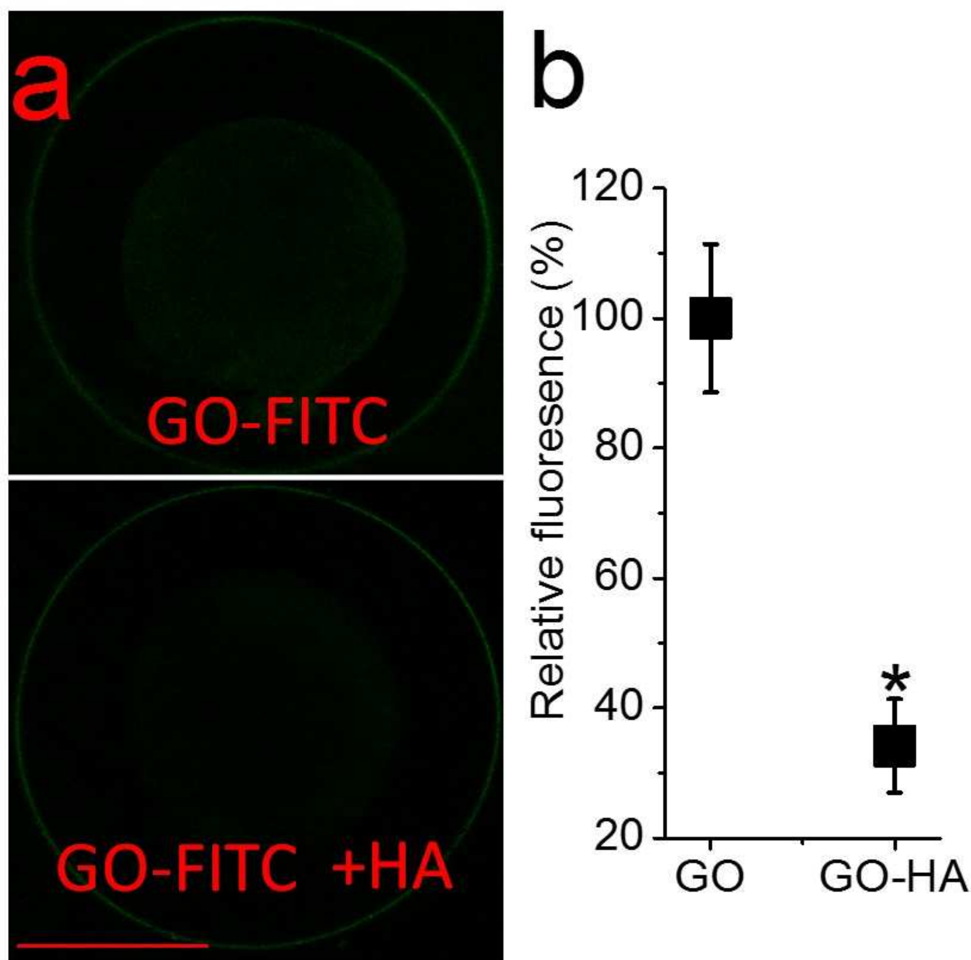

207

208 **Figure S10.** Uptake of GO *in vivo* when embryos developed over 16 h. (a) The
209 images of embryos exposed to 10 mg/L GO-FITC with or without HA. (b)
210 Semiquantitative analysis of GO in embryos was performed based on the relative
211 fluorescence using the software program Image J. GO-FITC, the fluorescein
212 isothiocyanate-labeled GO. GO, graphene oxide at 100 mg/L; HA, humic acid at 10
213 mg/L. Six images from three embryos in each treatment group. *, $p < 0.05$. The scale
214 bar is 450 μm in all images.

215

216

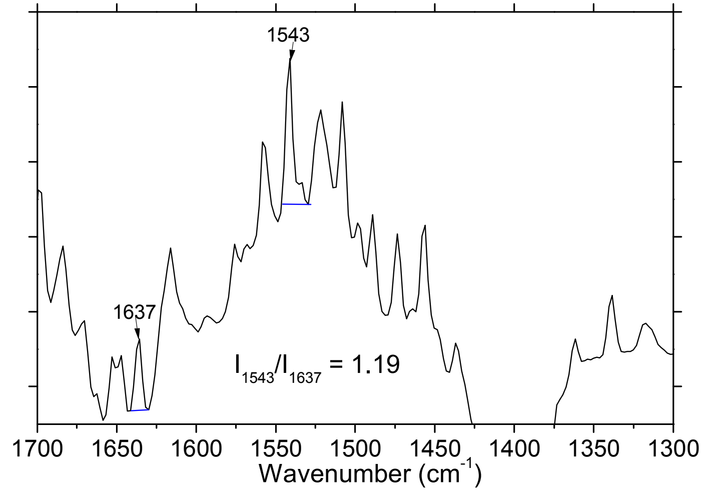

217 **Figure S11.** The overall protein pattern of the chorion at 4.0 °C without nanomaterial
218 exposure. There were 25 embryos in each treatment group, n = 3.
219

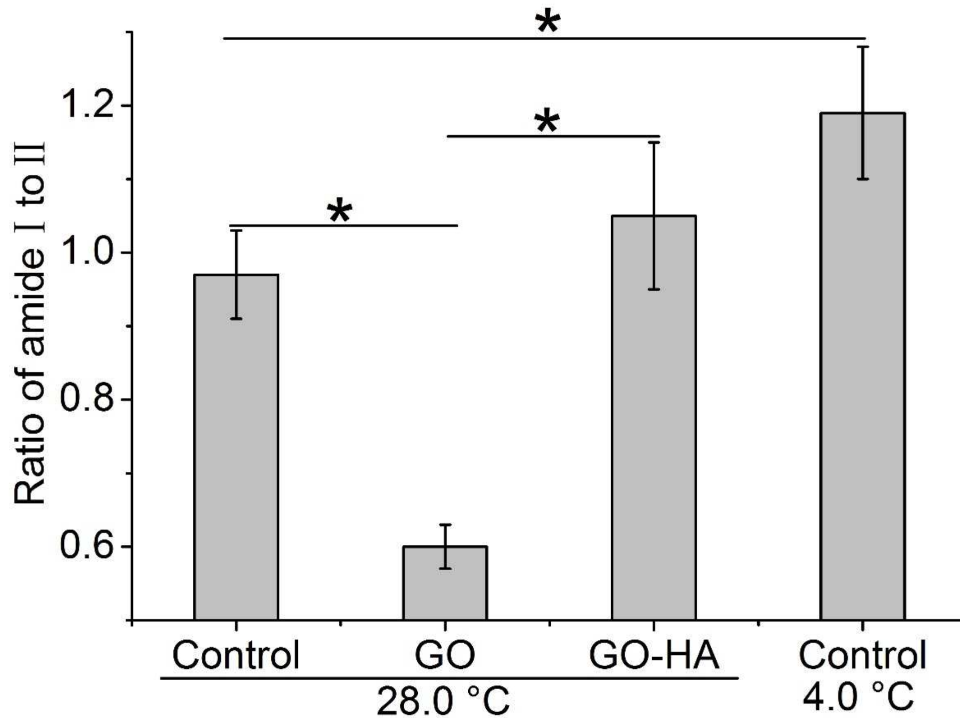

220
221 **Figure S12.** Overall protein pattern of the chorion. *****, significant at the $p < 0.05$ level,
222 $n = 3$. GO, graphene oxide at 100 mg/L; HA, humic acid at 10 mg/L. There were 25
223 embryos in each treatment group, n = 3.

224

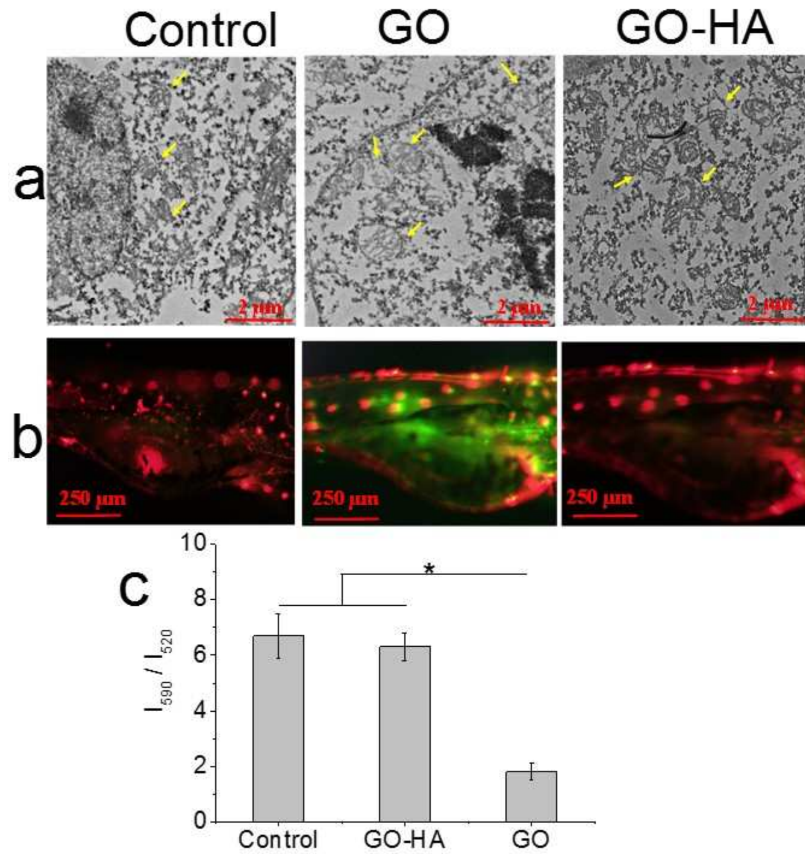

225

226 **Figure S13.** Mitochondrial toxicity of GO and GO−HA in zebrafish embryos. (a)
227 Transmission electron microscopy images of embryos. Blue arrows denote
228 mitochondria. (b) Fluorescence microscopy images of mitochondrial membrane
229 potential loss monitored by JC−1 staining. (c) Ratios of red to green fluorescence
230 intensity. A smaller ratio indicate a stronger mitochondrial membrane potential loss. *,
231 significant level at $p < 0.05$, n = 6. GO, graphene oxide at 100 mg/L. HA, humic acid
232 at 10 mg/L.
233

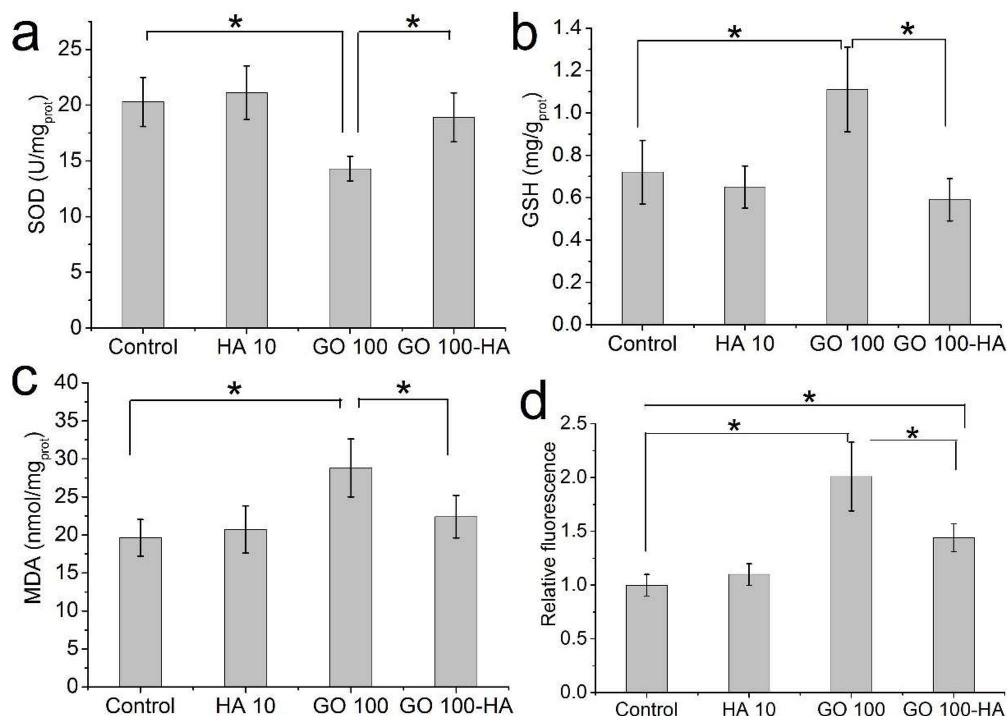

234

235 **Figure S14.** Oxidative stress of HA, GO and GO−HA on zebrafish embryogenesis at
236 72 hpf. (a) Activity of SOD. (b) Activity of GSH. (c) MDA content in zebrafish
237 embryos. (d) Relative ROS level represented by fluorescence intensity. Experiment
238 was conducted twice with 2 replicates per time, and 30 embryos per replicate. *,
239 significant level at $p < 0.05$. HA 10, humic acid at 10 mg/L. GO100, graphene oxide
240 at 100 mg/L. GO100−HA, mixture of 100 mg/L graphene oxide and 10 mg/L humic
241 acid. SOD, superoxide dismutase. GSH, glutathione. MDA, malondialdehyde. ROS,
242 reactive oxygen species.

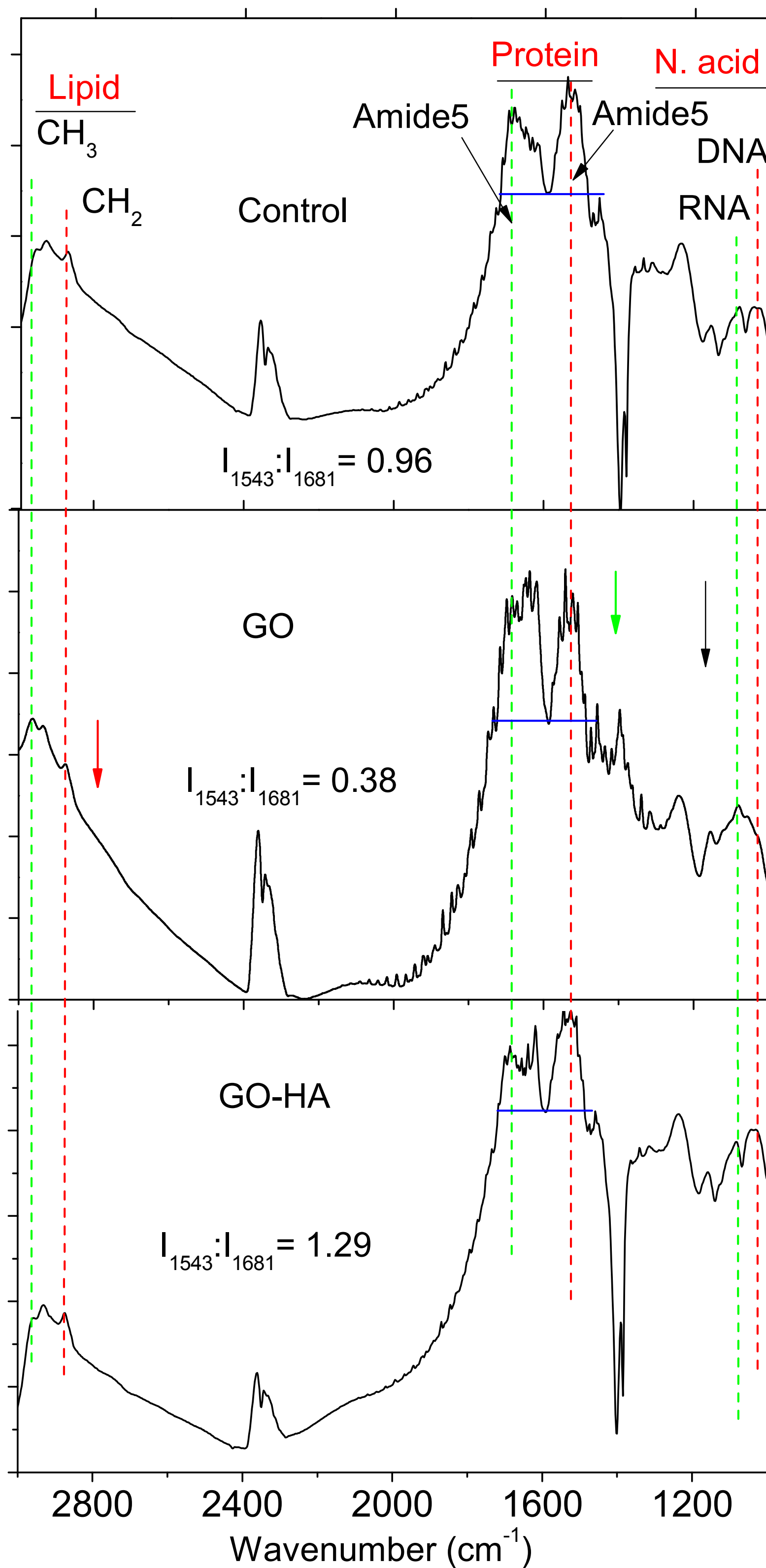

243

244 **Figure S15.** FT−IR spectra of zebrafish embryos treated with GO and GO−HA. GO,

245 graphene oxide at 100 mg/L. Red, green and black arrows denote the variation of
246 $-CH_2$, amide II and DNA, respectively. N. acid, nucleic acid. GO, graphene oxide at
247 100 mg/L. HA, humic acid at 10 mg/L. 25 embryos each treated groups, n = 3.
248

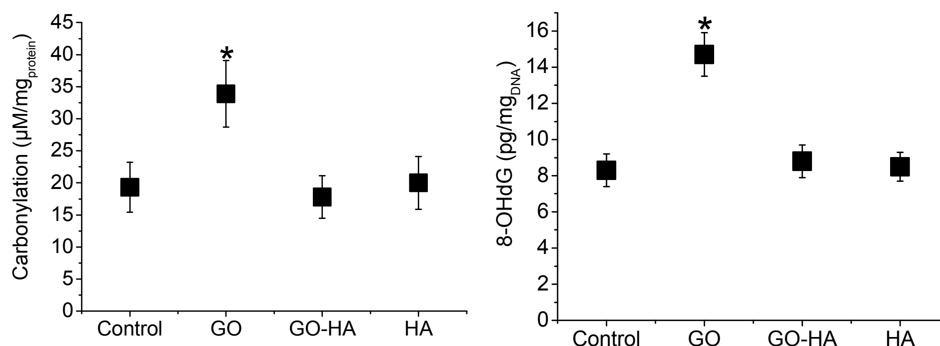

249
250 **Figure S16.** Effects of GO, GO-HA and HA on protein carbonylation and
251 8-hydroxy-2-deoxy-guanosine in embryos at 96 hpf. The experiment was conducted
252 two times with 60 embryos each time. *, significant level at $p < 0.05$ compared with
253 the control. HA : 10 mg/L humic acid; GO: graphene oxide at 100 mg/L.
254

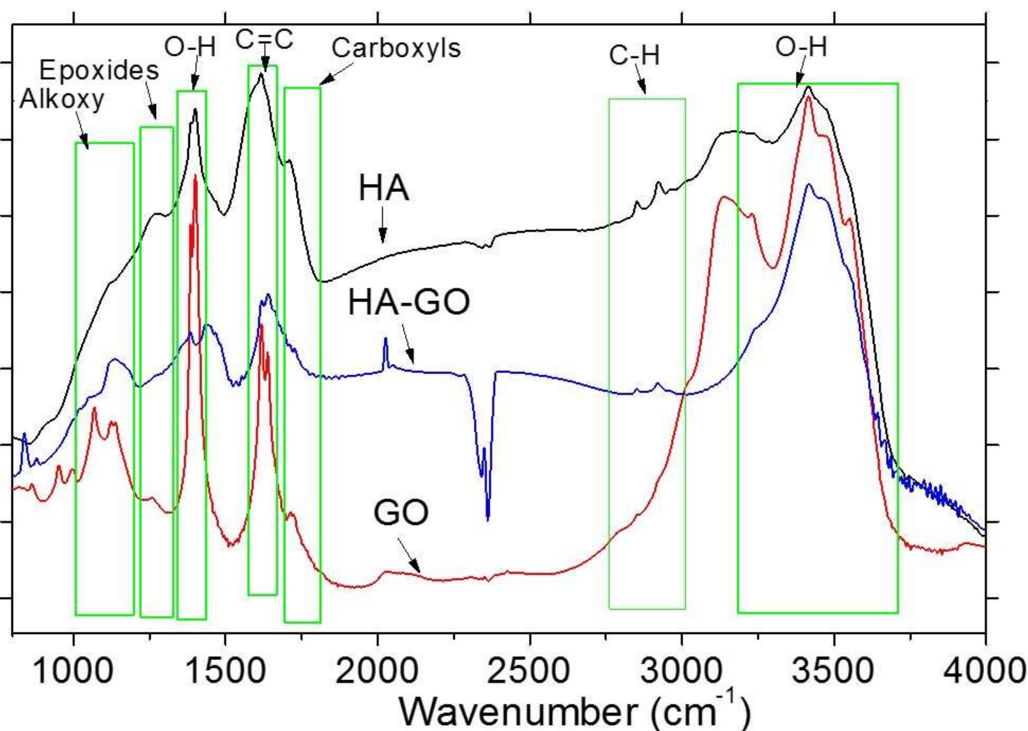

255
256 **Figure S17.** The FT−IR spectra of HA, GO and GO−HA. GO, graphene oxide at 100
257 mg/L. HA, humic acid at 10 mg/L.
258

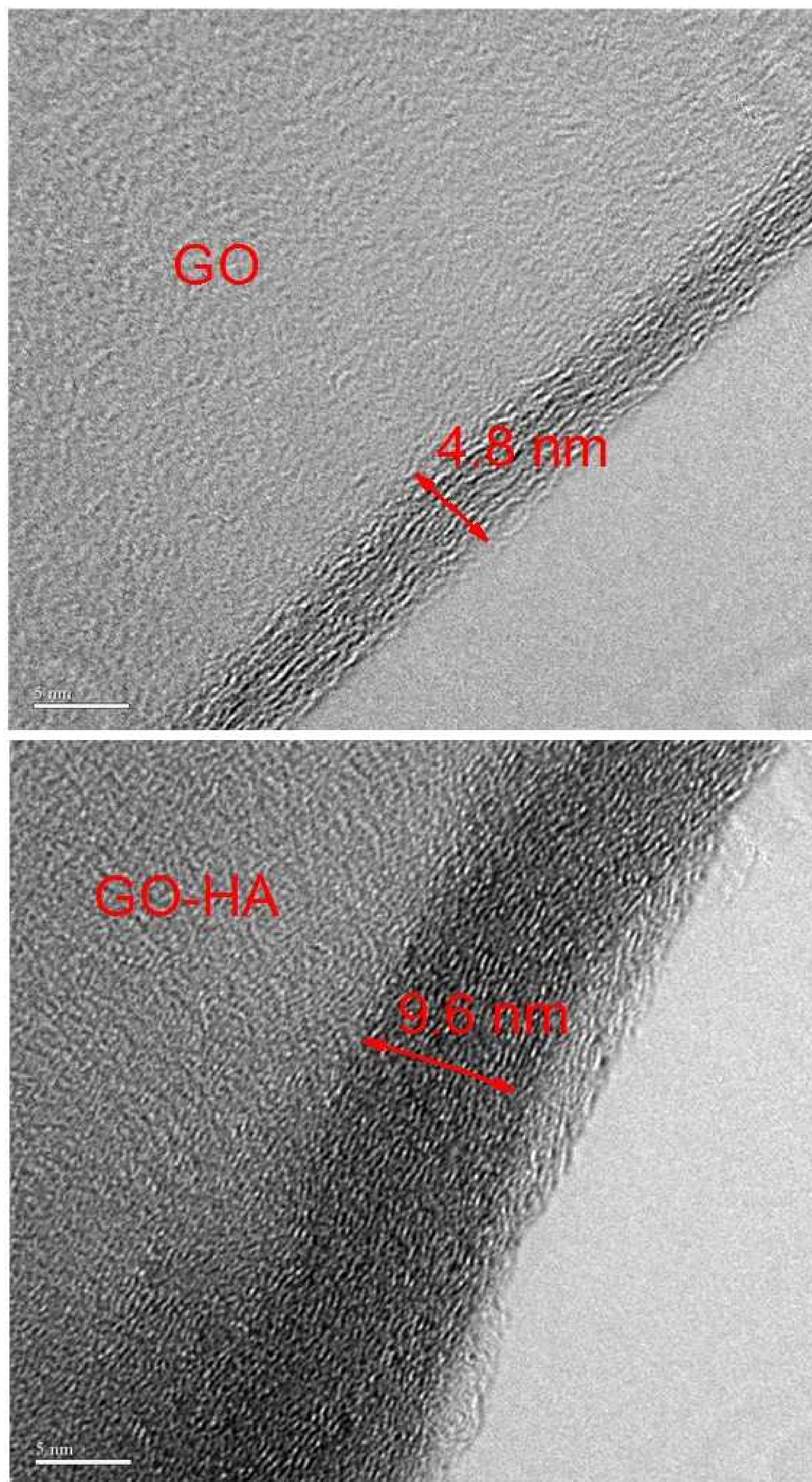

259

260 **Figure S18.** Transmission electron microscopy images of GO and GO−HA. GO,
261 graphene oxide. HA, humic acid.
262